THE JOURNAL OF BIOLOGICAL CHEMISTRY
Vol. 278, No. 44, Issue of October 31, pp. 43340–43345, 2003
Printed in U.S.A.

Physical Interactions of the Peroxisomal Targeting Signal 1 Receptor Pex5p, Studied by Fluorescence Correlation Spectroscopy*

Received for publication, July 18, 2003, and in revised form, August 20, 2003
Published, JBC Papers in Press, August 20, 2003, DOI 10.1074/jbc.M307789200

Dongyuan Wang‡, Nina V. Visser‡, Marten Veenhuis, and Ida J. van der Klei‡§

From Eukaryotic Microbiology, Groningen Biomolecular Sciences and Biotechnology Institute, University of Groningen, P.O. Box 14, 9750AA, Haren, The Netherlands

We have studied *Hansenula polymorpha* Pex5p and Pex8p using fluorescence correlation spectroscopy (FCS). Pex5p is the Peroxisomal Targeting Signal 1 (PTS1) receptor and Pex8p is an intraperoxisomal protein. Both proteins are essential for PTS1 protein import and have been shown to physically interact. We used FCS to analyze the molecular role of this interaction. FCS is a very sensitive technique that allows analysis of dynamic processes of fluorescently marked molecules at equilibrium in a very tiny volume. We used this technique to determine the oligomeric state of both peroxins and to analyze binding of Pex5p to PTS1 peptides and Pex8p. HpPex5p and HpPex8p were overproduced in *Escherichia coli*, purified by affinity chromatography, and, when required, labeled with the fluorescent dye Alexa Fluor 488. FCS measurements revealed that the oligomeric state of HpPex5p varied, ranging from monomers at slightly acidic pH to tetramers at neutral pH. HpPex8p formed monomers at all pH values tested. Using fluorescein-labeled PTS1 peptide and unlabeled HpPex5p, we established that PTS1 peptide only bound to tetrameric HpPex5p. Upon addition of HpPex8p, a heterodimeric complex was formed consisting of one HpPex8p and one HpPex5p molecule. This process was paralleled by dissociation of PTS1 peptide from HpPex5p, indicating that Pex8p may play an important role in cargo release from the PTS1 receptor. Our data show that FCS is a powerful technique to explore dynamic physical interactions that occur between peroxins during peroxisomal matrix protein import.

Peroxisomes are single membrane-bound organelles that are present in most aerobic eukaryotic cells. They acquire their matrix proteins by uptake of newly synthesized proteins from the cytosol. This process occurs predominantly via two pathways that rely on either of two conserved peroxisomal targeting signals (PTS1[1] and PTS2). The vast majority of matrix proteins contain a PTS1 that consists of a tripeptide motif (SKL or variants thereof) located at the extreme C terminus of the protein. *PEX* genes are essential for peroxisome biogenesis and have been numbered 1 to 29 according to the order of description (extensively reviewed in Ref. 1). Most of them encode proteins, designated peroxins, that play a role in peroxisomal matrix protein import.

The *PEX5* gene encodes the PTS1 receptor, Pex5p, which binds newly synthesized PTS1 proteins in the cytosol. This receptor is proposed to be translocated together with its cargo into the peroxisomal matrix (2). Dammai and Subramani (3) presented compelling evidence that human Pex5p, indeed, cycles between these two subcellular compartments.

Pex8p is the only known intraperoxisomal peroxin involved in matrix protein import. It is not required for association of Pex5p at the receptor docking complex on the peroxisomal membrane (4) but is important at a later stage in the import process. Recently, Agne *et al.* (5) showed that ScPex8p is important for the association of the receptor docking complex (comprising Pex14p and Pex17p) with another membrane-bound complex that contains the ring finger proteins Pex2p, Pex10p, Pex12p. Both membrane-bound protein complexes are involved in matrix protein import and possibly only function upon connection by Pex8p at the trans-site of the peroxisomal membrane (5).

Results of two-hybrid analysis and co-immune precipitations in *Saccharomyces cerevisiae* revealed that ScPex8p also physically interacts with ScPex5p in the organellar matrix (4). The molecular role of this interaction is still unknown. Most known Pex8 proteins contain a PTS1. However, the PTS1 of Pex8p is not the sole potential site of interaction with Pex5p, because this interaction is still robust when the PTS1 is removed (4). Most likely, the PTS1 of Pex8p is involved in targeting of the protein to peroxisomes instead of being important for its ultimate role in PTS1 matrix protein import.

To understand the molecular role of the physical interaction between Pex5p and Pex8p in matrix protein import, we studied these peroxins using a novel approach in peroxisome research, namely fluorescence correlation spectroscopy (FCS). FCS is a very sensitive technique developed for the study of dynamic processes of fluorescently labeled molecules at equilibrium in a tiny "volume" (6–8). FCS was developed in the mid-1970s but has only recently been recognized as a powerful tool in various areas of research. In FCS measurements, fluorescence intensity fluctuations are recorded only from those molecules that diffuse through an open volume element created by a focused laser beam. The time required for passage of molecules through this volume element is determined by the diffusion time, which is inversely proportional to the diffusion coefficient that is related to the size of the molecule. Thus, diffusion constants obtained from the analysis of fluorescence intensity fluctuations allow differentiation between relatively small, rapidly diffusing molecules and larger, more slowly diffusing ones.

Advantages of FCS over the techniques that are generally used to study protein-protein interactions (yeast two-hybrid analysis, GST pull-down experiments, co-immune precipitations) is that the size of protein complexes can be estimated,

* The costs of publication of this article were defrayed in part by the payment of page charges. This article must therefore be hereby marked "*advertisement*" in accordance with 18 U.S.C. Section 1734 solely to indicate this fact.

‡ Supported by Netherlands Organization for Scientific Research.

§ To whom correspondence should be addressed. Tel.: 31-50-363-2179; Fax: 31-50-363-8280; E-mail: I.J.van.der.Klei@biol.rug.nl.

[1] The abbreviations used are: PTS, peroxisomal targeting signal; FCS, fluorescence correlation spectroscopy; Fl, fluorescein.

allowing prediction of the stoichiometry of the interacting components. In addition, the fraction of free and bound molecules at equilibrium can be determined. Moreover, the proteins to be studied are not immobilized and the measurements are performed at relatively low protein concentrations (nM range), which reduces the risk of nonspecific aggregation.

In this study we analyze the interactions between purified *Hansenula polymorpha* Pex5p (9) and Pex8p (10) and synthetic PTS1 peptides *in vitro*. In each experiment one of these components was fluorescently labeled and analyzed by FCS. Calculation of the diffusion constants of the fluorescent molecule allowed us to determine the oligomeric state of the individual proteins and the physical interactions between these molecules. Our studies indicate that FCS is a powerful technique to explore the dynamics of physical interactions that occur during peroxisomal matrix protein import.

EXPERIMENTAL PROCEDURES

Peptides and Proteins—Peptides PTS1 (ASKL-COOH) and Fl-PTS1 (ASSASKL-COOH covalently bound to fluorescein (Fl) at the N terminus) were purchased from Eurosequence (Groningen, the Netherlands). The concentration of Fl-PTS1 was determined spectrophotometrically using a molar extinction coefficient $\epsilon_{480} = 7.8 \times 10^4$ M cm^{-1}.

For HpPex5p purification, a carboxyl-terminal His_6-tagged version was overproduced in *E. coli*. A *PEX5* PCR product, obtained using primers 5′-GCGCCATGGCATTTCTGGGAGGATCGG-3′and 5′-GCAGATCTTATGTCGTAGGTTTTTCGG-3′ was cloned as a 1.7-kb *Nco*I–*Bgl*II fragment (sites introduced by PCR) into vector pQE-60 (Qiagen, Hilden, Germany). The resulting plasmid was designated pQE60-*PEX5-HIS6*. For overproduction of carboxyl-terminal His_6-tagged HpPex8p, a *PEX8-HIS6* PCR product was obtained using primers 5′-CCTAGCATGCAGCCGTGGTACC-3′ and 5′-CGCAGATCTTAATTTTGCTTTTTCCTGACTCTC-3′ and cloned into vector pQE-70. The resulting plasmid was designated pQE70-*PEX8-HIS6*.

Both plasmids (pQE60-*PEX5-HIS6* and pQE70-*PEX8-HIS6*) were transformed to *E. coli* M15 (pREP4). Transformants were grown as detailed in the QIA*expressionist*™. Overproduction was induced by addition of 1 mM isopropyl-1-thio-β-D-galactopyranoside and incubation for 3 h at 30 °C. All subsequent steps were performed at 4 °C. Cells were harvested by centrifugation and resuspended in 50 mM phosphate buffer, pH 7.0, containing 300 mM NaCl, 1% Tween 20, 10% glycerol, 0.2 mM β-mercaptoethanol, 1 mM phenylmethylsulfonyl fluoride, complete™ protease inhibitor (Roche Applied Science), 50 μg/ml DNase, and 100 μg/ml RNase and subsequently broken using a French Press. Cell debris and other insoluble material were removed by centrifugation (10,000 × *g*, 20 min). Supernatants were incubated for 1 h with nickel-nitrilotriacetic acid resin (500 mg protein/ml resin; Qiagen) followed by extensive washing with buffer A (50 mM phosphate buffer, pH 7.0, containing 100 mM NaCl) with increasing concentrations of imidazole (up to 40 mM), followed by elution with buffer A containing 200 mM imidazole. Pex5p or Pex8p peak fractions, determined by Western blotting using anti-Pex5p or anti-Pex8p antibodies, were further purified by anion exchange chromatography (MonoQ; Amersham Biosciences) using a linear gradient of 0.1–1 M NaCl in 20 mM Bis-Tris-HCl buffer (pH 7.0) for HpPex5p and in 20 mM Tris-HCl buffer (pH 7.8) for HpPex8p. HpPex5p was further purified by gel filtration chromatography (Superose 12; Amersham Biosciences) in buffer A containing 300 mM NaCl. HpPex5p and HpPex8p were labeled with Alexa Fluor 488 using the protein labeling kit of Molecular Probes (Leiden, The Netherlands) and dialyzed against buffer prior to the FCS measurements. Dialysis did not prevent the presence of residual free Alexa Fluor 488 in the samples.

Analysis of the Functionality of HpPex5p-His$_6$ and HpPex8p-His$_6$—The functionality of carboxyl-terminal His_6-tagged HpPex5p was tested by introducing the *HpPEX5-HIS6* gene under control of the endogenous promoter (P_{PEX5}) in a *H. polymorpha PEX5* deletion strain (Δ*pex5*) (9). To this purpose the *PEX5-HIS6* cassette was isolated as a 1.8-kb *Nco*I (blunted)-*Hin*dIII fragment from the pQE60-*PEX5-HIS6* plasmid and ligated into the shuttle vector pHS5 together with a 0.5-kb *Bam*HI (blunted) *Sac*I *PEX5* promoter fragment (*Bam*HI site introduced by PCR). The resulting plasmid was transformed to *H. polymorpha* Δ*pex5*.

The functionality of carboxyl-terminal His_6-tagged HpPex8p was determined by integrating the carboxyl-terminal part of the *HpPEX8-HIS6* gene of pQE70-*PEX8-HIS6* in *H. polymorpha* NCYC495 *leu 1.1* in such a way that only HpPex8p-His_6 is produced. To this purpose the carboxyl-terminal part of *PEX8-HIS6* was isolated as a 1.3-kb *Hin*dIII fragment from pQE70-*PEX8-HIS6* and ligated in vector pHS5 digested with *Hin*dIII. The resulting plasmid was linearized with *Mlu*I and transformed to *H. polymorpha* NCYC495 *leu 1.1*. Prototrophic transformants were selected. The synthesis of His_6-tagged HpPex5p and His_6-tagged HpPex8p in the two constructed strains was determined by Western blot analysis using monoclonal antibodies against the histidine tag (Dianova GmbH, Hamburg, Germany). In addition, these strains were tested for their ability to grow on methanol, which is indicative for normal peroxisome formation (9, 10).

FCS—Protein concentrations were calculated from the absorption at 280 nm, using molar extinction coefficients of 5.8×10^4 M cm^{-1} for HpPex5p and 9.3×10^4 M cm^{-1} for HpPex8p calculated from their aromatic amino acid content. For binding studies, samples were preincubated at 37 °C for 1 h prior to the measurements.

A ConfoCor 1 FCS setup (Zeiss, Göttingen, Germany) (8, 11), equipped with an argon ion laser line of 488 nm and a 40 × 1.2 water immersion apochromat objective, was used in all experiments. The light intensity was adjusted by using various neutral density filters. As a sample carrier, a 96-well chamber was used. The pinhole was adjusted to 40 μm; the alignment and focusing of the setup were frequently checked by measuring the photon count traces of 10 nM Rhodamine 110. Autocorrelation traces were acquired during 30 or 60 s and repeated 10 times. All the experiments were conducted at room temperature. The autocorrelation curves were globally analyzed to a model consisting of diffusion and triplet state (12) as shown in Equation 1

$$G(\tau) = 1 + \frac{1}{\langle N \rangle} \cdot \frac{1 - T + Te^{-\tau/\tau_T}}{(1-T)} \sum_j \alpha_j \cdot \frac{1}{\left(1 + \frac{\tau}{\tau_{\mathrm{dif},j}}\right)\sqrt{1 + \left(\frac{\omega_{xy}}{\omega_z}\right)^2 \frac{\tau}{\tau_{\mathrm{dif},j}}}} \quad \text{(Eq. 1)}$$

where $\langle N \rangle$ is the average number of molecules, T is the fraction of molecules in the triplet state, and $1/\tau_T$ the corresponding triplet decay rate, $\tau_{\mathrm{dif},j}$ is the diffusion time of molecular species j, ω_{xy} and ω_z are the equatorial and axial radii of the confocal volume set up by the laser beam, and ω_z/ω_{xy} is the structural parameter. Equation 1 is written in a multicomponent form with α_j the fraction of molecular species j. In Equation 1 it is assumed that all species have the same triplet characteristics and molecular brightness. The dimensions of the confocal detection volume and the structural parameter are obtained from global analysis of the autocorrelation curves of the standard Rhodamine 110 in water having a diffusion constant of 280 $\mu m^2 s^{-1}$ (13).

In global analysis several correlation functions are combined in one data set and simultaneously fitted with certain parameters linked over the set, ensuring more reliable parameter recovery and thus more consistent representation of the physical processes under investigation (14). All the experimental autocorrelation curves were globally fitted by the theoretical autocorrelation function given in Equation 1 using the FCS data processor 1.3 of the Scientific Software Technologies Center of Belarusian State University, Belarus. The quality of the fits and performance of the optimization methods was improved by fixing the parameters that are known *a priori* from independent experiments (for instance, free Alexa Fluor 488).

The relation between diffusion time and diffusion constant is shown in Equation 2.

$$\tau_{\mathrm{dif}} = \frac{\omega_{xy}^2}{4D} \quad \text{(Eq. 2)}$$

In Tables I and II diffusion constants D are used, because these are absolute numbers independent of the size of the confocal detection volume. The diffusion coefficient of a spherical particle scales inversely to the hydrodynamic radius r_h of the particle according to the Stokes-Einstein relation as shown in Equation 3

$$r_h = \frac{kT}{6\pi\eta D} \quad \text{(Eq. 3)}$$

where η is the viscosity, T the absolute temperature, and k the Boltzmann constant. Assuming that r_h of the particle is proportional to the cubic root of its molecular mass M, D can be rewritten as shown in Equation 4.

$$D^{-1} \approx \frac{6\pi\eta}{kT} \sqrt[3]{M} \quad \text{(Eq. 4)}$$

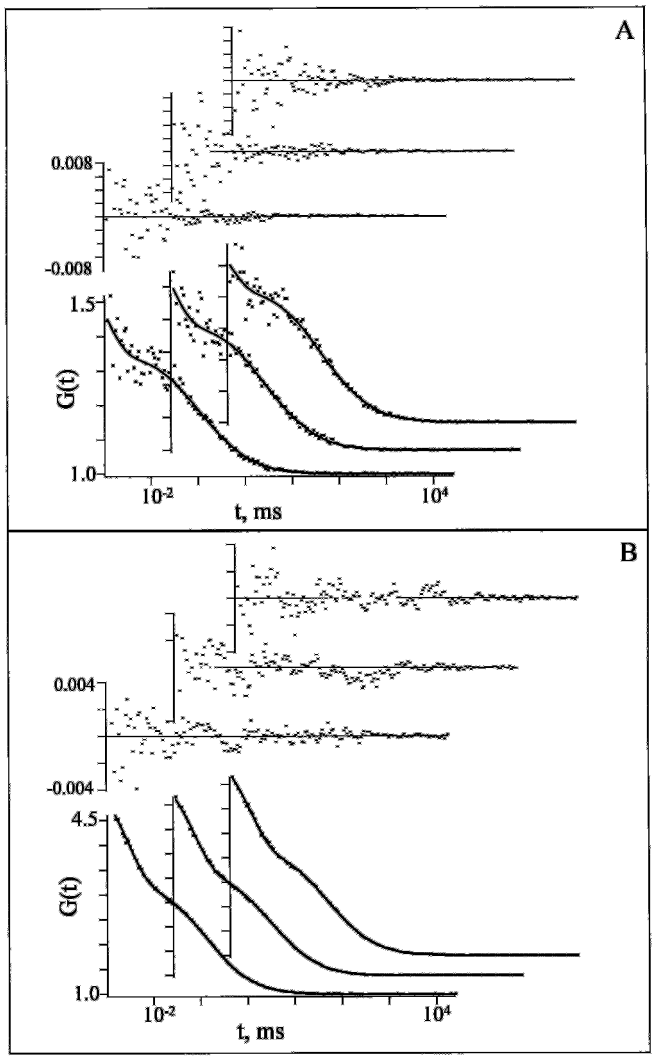

FIG. 1. **Examples of experimental autocorrelation curve (*dots*), fitted (*solid line*), and residuals (*upper inset*) of HpPex5p labeled with Alexa Fluor 488 at pH 7.2 (*A*) and 6.0 (*B*).** In all the experiments the concentration of HpPex5p was 50 nM. After global analysis of 10 experimental curves to the model of Equation 1, the following parameters were obtained. *A*, τ_t = 3.2 μs, T ≈ 40%; Alexa-free τ_{dif} = 64 μs (fixed); HpPex5p τ_{dif} = 467 μs (confidence limit: 432–503 μs). *B*, τ_t = 2.9 μs, T ≈ 40%; Alexa-free τ_{dif} = 64 μs (fixed); HpPex5p τ_{dif} = 292 μs (265–324 μs).

Assuming a more or less globular shape of the molecules, Equation 4 allows us to derive the molecular mass of a protein by comparing it with the known molecular mass of a reference compound.

RESULTS

The Oligomeric States of HpPex5p—Because of the various oligomeric states of Pex5p that have been reported (15–17), ranging from monomers to tetramers, we initiated our studies by analyzing the oligomeric state of Pex5p. To facilitate purification, a carboxyl-terminal His_6-tagged version of *H. polymorpha* Pex5p (HpPex5p) was overproduced in *E. coli*. The His_6-tagged HpPex5p was fully functional because synthesis of this protein in a *H. polymorpha PEX5* deletion strain fully restored the capacity of the cells to grow on methanol (data not shown).

Purified HpPex5p was labeled with the fluorescent dye Alexa Fluor 488, which enabled us to follow the fate of the protein in solution using FCS. In Fig. 1 examples of three autocorrelation curves (of ten) are shown together with fitted curves and residuals. The autocorrelation curves were fitted globally to a diffusion model including triplet kinetics (see "Experimental Procedures"). The best fit was achieved when a two-component diffusion model was used, where the diffusion time of free Alexa Fluor 488 was fixed to the earlier estimated value. A rigorous error analysis at a confidence interval of 67% for the diffusion time of HpPex5p was performed (14). The diffusion constant of HpPex5p at pH 7.2 (see Fig. 1*A*) appeared to be 38 $\mu m^2 s^{-1}$ (with confidence limits 36–41 $\mu m^2 s^{-1}$). This diffusion constant corresponds to a molecular mass of ~250 kDa (198–312 kDa), assuming that the protein has a globular shape (see Equation 4 under "Experimental Procedures"). Because the molecular mass of HpPex5p calculated from its amino acid sequence amounts to 63.9 kDa (9), we conclude that the protein formed tetramers under the prevailing experimental conditions. At pH 6.0 (Fig. 1*B*), the diffusion constant of HpPex5p increased to a value that corresponds to a molecular mass of 61 kDa (48–83 kDa), indicative of a monomeric conformation. These data indicate that the oligomeric state of HpPex5p is dependent on the pH and varies within a relatively small pH interval.

PTS1 Peptides Predominantly Bind to Tetrameric HpPex5p—In order to study binding of a peptide containing the consensus sequence (*SKL)* of the PTS1, a chemically synthesized peptide (ASSA*SKL*) was labeled with fluorescein (Fl-PTS1). Autocorrelation curves in the presence and absence of HpPex5p were collected. These experiments were conducted at two different pH values. In Fig. 2*A* three autocorrelation curves (of ten) are shown together with fitted curves and residuals for Fl-PTS1 at pH 7.2. A single diffusion constant of 224 $\mu m^2 s^{-1}$ (206–239 $\mu m^2 s^{-1}$) was obtained at pH 7.2 (Fig. 2*A*). At pH 6.0, a similar value was obtained (data not shown). In Fig. 2*B* the same set of curves is presented for Fl-PTS1 in the presence of HpPex5p at pH 7.2. The best fit was obtained when a two-component diffusion model was used in which the diffusion time of free Fl-PTS1 was fixed in the analysis. In the presence of HpPex5p the autocorrelation curve shifted to longer diffusion times, indicating binding of the peptide to a larger molecule (Fig. 2*B* legend and Table I). At the experimental conditions used, the two-component diffusion model revealed that 14% of the peptide was bound to HpPex5p. The diffusion constant of the bound PTS1 peptide corresponded to a molecular mass of ~277 kDa, indicating that it was bound to tetrameric HpPex5p. In an identical experiment performed at pH 6.0 (data not shown), only the short diffusion time corresponding to free Fl-PTS1 was observed, and no additional diffusion time could be distinguished. This indicates that no significant binding of the PTS1 peptide to HpPex5p occurs at this pH.

In control experiments performed at both pH values using purified HpPex8p (see below), only the short diffusion time of the free peptide could be recovered. Hence, the PTS1 peptide specifically binds to HpPex5p but not to HpPex8p.

HpPex5p Interacts with HpPex8p—So far, no data have been reported on the oligomeric state of Pex8p. To facilitate purification, His_6-tagged HpPex8p was overproduced in *E. coli*. The functionality of the tagged protein was analyzed using a constructed strain that produces only the His_6-tagged version of Pex8p under control of the endogenous promoter. Cells of this strain grew normally on methanol, indicating that the protein was fully functional (data not shown).

Purified HpPex8p was labeled with Alexa Fluor 488. Experimental autocorrelation curves of labeled HpPex8p were obtained at different pH values. These curves fitted best with a two-component diffusion model, one corresponding to free Alexa Fluor 488 and the other to Alexa Fluor 488-labeled HpPex8p (data not shown). After applying the same strategy of analysis as described above, the diffusion constants presented in Table II were recovered. The molecular mass of HpPex8p, calculated from the diffusion constant, amounted to 60 (pH

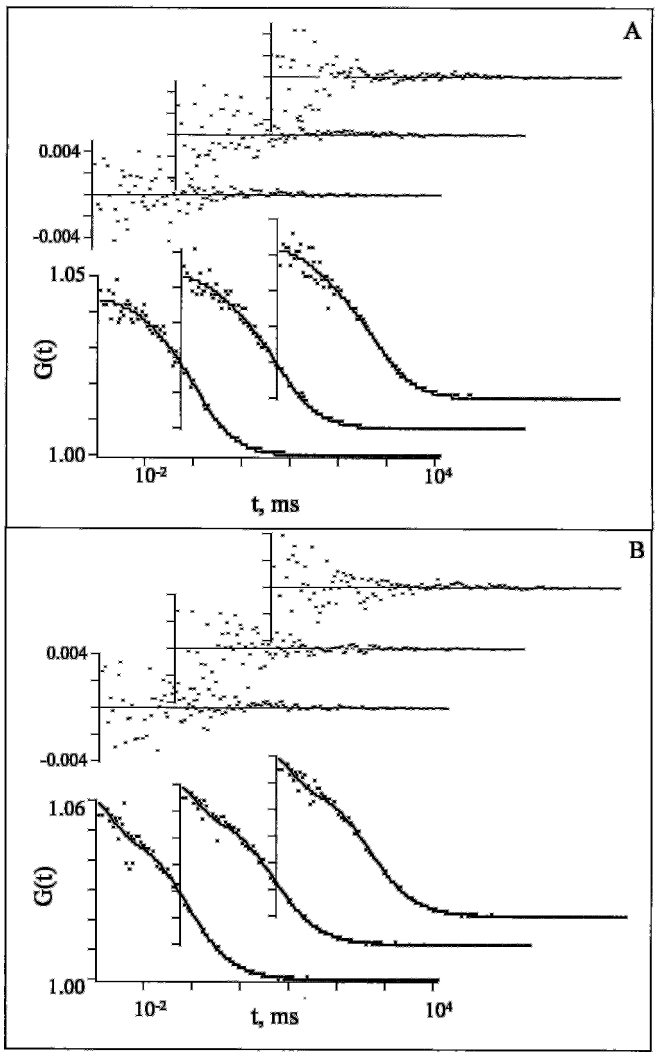

FIG. 2. **Examples of experimental autocorrelation curve (*dots*), fitted (*solid line*), and residuals (*upper inset*) of Fl-PTS1 in the absence (*A*) or presence (*B*) of HpPex5p at pH 7.2.** The concentration of Fl-PTS1 was 50 nM. HpPex5p was used at a concentration of 10 nM. After global analysis of 10 experimental curves to the model of Equation 1, the following parameters were obtained. *A*, one-component fit: τ_t = 3.1 μs, T ≈ 10%; Fl-PTS1-free τ_{dif} = 80 μs (75–86 μs). *B*, two-component fit: τ_t = 1.7 μs, T ≈ 10%; Fl-PTS1-free τ_{dif} = 80 μs (fixed); HpPex5p τ_{dif} = 479 μs (424–521 μs).

TABLE I
Diffusion constants of fluorescein-labeled PTS1-peptide in the presence of HpPex5p with and without HpPex8p

The measurements were performed at pH 7.2. The concentration of Fl-PTS1 was 50 nM, HpPex5p 10 nM, and HpPex8p 300 nM.

	Diffusion constant	Calculated molecular mass	Fraction of Fl-PTS1 bound to HpPex5p
	$\mu m^2 s^{-1}$	*kDa*	%
Fl-PTS1	224 (206–239)	1.1 (1.06–.65)	
Fl-PTS1 + HpPex5p	37 (34–42)	277 (202–375)	14 ± 1
Fl-PTS1 + HpPex5p + HpPex8p	37 (fixed)	277 (202–375)	9 ± 1

8.0)-73 kDa (pH 6), which is similar to the mass calculated from its amino acid composition (77 kDa) (10). We therefore conclude that purified HpPex8p occurs as a monomer independent of the pH.

Upon addition of excess unlabeled HpPex5p to the Alexa Fluor 488-labeled HpPex8p solution (at pH 7.2), again a good two-component fit was obtained. After fixing the diffusion time of free Alexa Fluor 488 dye, a diffusion constant of ~49 $\mu m^2 s^{-1}$ was obtained (Table II). This value corresponds to a molecular mass of ~127 kDa and suggests the formation of heterodimeric complexes of HpPex8p and HpPex5p. Under these conditions (*i.e.* a 10-fold molar excess of HpPex5p), most HpPex8p was bound to HpPex5p. Similar results were obtained when the experiments were performed at pH 6.0 or 8.0 (Table II).

TABLE II
Diffusion constants of Alexa-labeled HpPex8p at different pH values, in the presence and absence of HpPex5p and PTS1 peptide

The concentration of Alexa Fluor 488-labeled HpPex8p was 50 nM, the HpPex5p concentration was 500 nM, and the PTS1 peptide concentration was 5 μM.

PH	Proteins	PTS1 peptide	Diffusion constant	Calculated molecular mass
			$\mu m^2 s^{-1}$	*kDa*
6.0	HpPex8p	−	58 (53–64)	73 (54–95)
6.0	HpPex8p + HpPex5p	−	45 (42–49)	157 (122–197)
6.0	HpPex8p + HpPex5p	+	47 (46–50)	135 (118–152)
7.2	HpPex8p	−	61 (58–65)	63 (52–73)
7.2	HpPex8p + HpPex5p	−	49 (46–51)	127 (106–149)
7.2	HpPex8p + HpPex5p	+	45 (42–49)	158 (124–196)
8.0	HpPex8p	−	70 (65–76)	60 (47–75)
8.0	HpPex8p + HpPex5p	−	51 (47–55)	154 (121–183)
8.0	HpPex8p + HpPex5p	+	53 (48–59)	139 (100–185)

Upon addition of excess (500 nM) unlabeled HpPex8p to the mixture, the diffusion constant increased again (data not shown), indicating that indeed the high molecular mass species represented dimers consisting of labeled HpPex8p and unlabeled HpPex5p. Addition of labeled HpPex8p (50 nM) to a mixture of HpPex5p (500 nM) and PTS1 peptide (5 μM) resulted in a similar autocorrelation curve, indicating that the presence of PTS1 peptide did not influence the HpPex5p-HpPex8p interaction (Table II).

HpPex8p Causes Dissociation of the HpPex5p-PTS1 Peptide Complex—Next we tested whether HpPex8p affected binding of PTS1 peptide to HpPex5p. To test this, unlabeled HpPex8p (300 nM) was added to a mixture of unlabeled HpPex5p (10 nM) and fluorescein-labeled PTS1 peptide (50 nM) preincubated at 37 °C for 1 h. The experimental autocorrelation curves were best fitted with a two-component diffusion model, corresponding to free peptide and peptide bound to tetrameric HpPex5p. No significant amounts of the Fl-PTS1 peptide bound to HpPex5p-HpPex8p heterodimers could be detected. The addition of HpPex8p resulted in a decrease in the fraction of PTS1 peptide bound to tetrameric HpPex5p. At the experimental conditions used, the fraction of bound peptide decreased to 9% (compare with 14% that was bound in the absence of HpPex8p; Table I).

DISCUSSION

In this study we used FCS to study physical interactions of two peroxins, Pex5p and Pex8p, involved in peroxisomal matrix protein import. A wealth of experimental data has been reported showing peroxin-peroxin and receptor-PTS interactions (reviewed in Ref. 1). However, the techniques used (*e.g.* yeast two-hybrid analysis, co-immune precipitation, surface plasmon resonance analysis) do not allow determination of the stoichiometry or kinetics of these interactions. Here we show that FCS is a powerful tool to assess the dynamics of peroxin interactions. FCS is generally used to study binding of small ligands to relatively large structures (proteins, membranes). We show that FCS is also suitable to study the interactions of proteins of comparable molecular mass (*e.g.* HpPex5p and HpPex8p) when global analysis of many experimental data is applied. A major advantage of FCS is the use of low protein concentrations, which prevents the possible formation of nonspecific protein aggregates. Pex5p has been predicted to function as a cycling

receptor between the cytosol and the peroxisomal matrix. The carboxyl-terminal domain of HpPex5p contains tetratricopeptide repeats that are responsible for binding PTS1 signals, whereas the amino terminus interacts with several other peroxins (*e.g.* Pex13p, Pex14p, Pex12p). This part of the protein is also involved in Pex5p oligomerization (15).

In this study we showed that HpPex5p exists in different oligomeric conformations that vary with the pH. HpPex5p predominantly formed monomers at pH 6.0, whereas at pH 7.2 it is tetrameric. This observation may add to an explanation of the apparent conflicting data reported for mammalian Pex5p. Using gel filtration chromatography at pH 8.0, human Pex5p was found to be tetrameric (15), whereas for rat and Chinese hamster Pex5p it was concluded, based on similar experiments performed at pH 7.2 (17), that the protein formed dimers.

Only at pH 7.2 did PTS1 peptides bind to HpPex5p, indicating that ligand binding may be confined to tetramers. This finding is in line with the recently proposed "pre-implex" model for peroxisomal matrix protein import, which predicts that peroxisomal matrix protein import is mediated by tetrameric Pex5p molecules (18). The pre-implex model proposes that one Pex5p tetramer binds four PTS1 proteins in the cytosol. Because peroxisomal matrix proteins are often imported as oligomers that contain one PTS1 per subunit, very large protein complexes (the so-called pre-implexes) containing several Pex5p tetramers and different oligomeric PTS1 proteins may be formed prior to import (18).

Analysis of Pex5p-PTS1 binding revealed that at pH 7.2 14% of the peptide was bound to HpPex5p under the experimental conditions used. This corresponds to an equilibrium dissociation constant of ~18 nM, which is in the same range as reported for the carboxyl-terminal tetratricopeptide domain of human Pex5p, based on fluorescence anisotropy measurements (equilibrium dissociation constant 35–70 nM (19, 20)).

The apparent small fraction of bound peptide (14%) obtained under the experimental conditions used is because of the low protein and peptide concentrations (in the nanomolar range). In all measurements described in this study, the fluorescent molecule to be analyzed was present at a final concentration of 50 nM, which is suitable for FCS experiments. In FCS, the focused laser beam illuminates a very tiny volume element (~1 μm^3). To detect fluctuations in fluorescence due to diffusion of fluorescent molecules into and out of this volume element, it should contain, on average, not more than one fluorescent molecule, which is reached at concentrations in the nanomolar range (21).

It is likely that the proteins analyzed in this study are also functioning at low concentrations under physiological conditions. Because PTS1 protein import is very efficient, newly synthesized PTS1 proteins are generally not detectable in the cytosol. Also, HpPex5p is not an abundant component of the cytosol, and in peroxisomes both HpPex5p and HpPex8p are present at relatively low concentrations (9, 10).

Our results indicated that HpPex8p is monomeric. Using FCS, we could establish a physical interaction between HpPex5p and HpPex8p, namely the formation of heterodimers. The Pex5p-Pex8p interaction was previously reported for the bakers' yeast orthologs using two-hybrid analysis and co-immune precipitations (4). As for bakers' yeast, the interaction between HpPex5p and HpPex8p was not the result of binding of the PTS1 of HpPex8p to the tetratricopeptide domain of HpPex5p, because a His_6 tag was added to the carboxyl terminus of HpPex8p, thereby destroying its PTS1.

When HpPex8p was added to a solution of tetrameric HpPex5p that had bound PTS1 peptide, the fraction of bound PTS1 peptide significantly decreased. At the same time

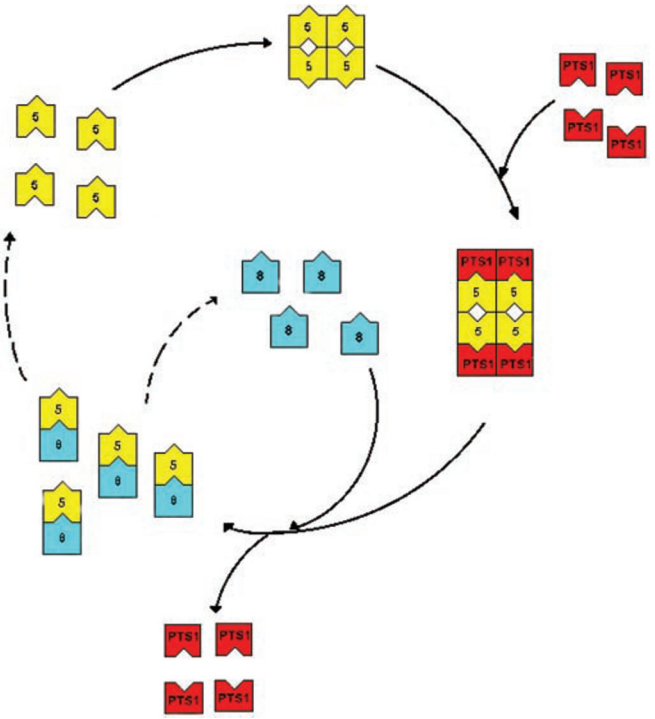

FIG. 3. **Hypothetical model of Pex5p and Pex8p interactions during one cycle of PTS1 protein import.** Tetrameric Pex5p binds four PTS1 proteins. After import, heterodimeric Pex5p-Pex8p complexes are formed and the PTS1 proteins are released. Subsequently, the Pex5p-Pex8p complex dissociates followed by tetramerization of Pex5p. Pex5p, *yellow*; PTS1-protein, *red*; Pex8p, *blue*. The *dashed line* represents dissociation of the Pex5p-Pex8p complex by an unknown mechanism.

HpPex8p-HpPex5p heterodimers were formed. Because binding of PTS1 peptide to HpPex8p-HpPex5p heterodimers could not be detected, it is likely that HpPex8p stimulates dissociation of HpPex5p tetramers, thereby causing the release of the PTS1 peptide.

Fig. 3 shows a hypothetical model in which our current data are included. In the cytosol (neutral pH) HpPex5p exists as a tetramer, which represents the preferred conformation for PTS1 binding. Gatto *et al.* (19) showed that the carboxyl-terminal tetratricopeptide domain of Pex5p is capable of binding one PTS1 peptide. Hence, up to four PTS1 peptides can bind to one Pex5p tetramer. The tetrameric HpPex5p cargo complex is imported into the peroxisomal matrix, where matrix-localized HpPex8p stimulates dissociation of the HpPex5p tetramers and release of the cargo, paralleled by HpPex5p-HpPex8p heterodimer formation. Dissociation of HpPex5p tetramers may be promoted by the slightly acidic pH in the peroxisomal matrix of *H. polymorpha* (22). How the HpPex5p-HpPex8p complex dissociates again is not known. According to the extended shuttle model, Pex5p will recycle to the cytosol, where Pex5p tetramers can facilitate another round of PTS1 protein import.

This is the first time that FCS has been used in peroxisomal research. Our data show that FCS is a powerful technique to obtain detailed insight into the molecular mechanisms of peroxisome biogenesis. The next challenge is to apply these studies *in vivo*, thereby focusing the laser beam in different cellular compartments to further test current models on peroxisomal matrix protein import. Using naturally occurring ligands (*e.g.* oligomeric PTS1 proteins), it may also allow us to put the recently postulated pre-implex model of matrix protein import to the test (18).

Acknowledgments—We thank Prof. A. J. W. G. Visser (MicroSpectroscopy Centre, Wageningen University, The Netherlands) for stimu-

lating discussions. The skillful assistance of Marcel Lunenborg is gratefully acknowledged.

REFERENCES

1. Purdue, P. E., and Lazarow, P. B. (2001) *Annu. Rev. Cell Dev. Biol.* **17,** 701–752
2. Van der Klei, I. J., and Veenhuis, M. (1996) *Ann. N. Y. Acad. Sci.* **804,** 47–59
3. Dammai, V., and Subramani, S. (2001) *Cell* **105,** 187–196
4. Rehling, P., Skaletz-Rorowski, A., Girzalsky, W., Voorn-Brouwer, T. M., Franse, M. M., Distel, B., Veenhuis, M., Kunau, W. H., and Erdmann, R. (2000) *J. Biol. Chem.* **275,** 3593–3602
5. Agne, B., Meindl, N. M., Niederhoff, K., Einwachter, H., Rehling, P., Sickmann, A., Meyer, H. E., Girzalsky, W., and Kunau, W. H. (2003) *Mol. Cell* **11,** 635–646
6. Medina, M. A., and Schwille, P. (2002) *Bioessays* **24,** 758–764
7. Hess, S. T., Huang, S., Heikal, A. A., and Webb, W. W. (2002) *Biochemistry* **41,** 697–705
8. Hink, M. A., Borst, J. W., and Visser, A. J. W. G. (2003) *Methods Enzymol.* **361,** 93–112
9. Van der Klei, I. J., Hilbrands, R. E., Swaving, G. J., Waterham, H. R., Vrieling, E. G., Titorenko, V. I., Cregg, J. M., Harder, W., and Veenhuis, M. (1995) *J. Biol. Chem.* **270,** 17229–17236
10. Waterham, H. R., Titorenko, V. I., Haima, P., Cregg, J. M., Harder, W., and Veenhuis, M. (1994) *J. Cell Biol.* **127,** 737–749
11. Hink, M. A., Griep, R. A., Borst, J. W., van Hoek, A., Eppink, M. H., Schots, A., and Visser, A. J. W. G. (2000) *J. Biol. Chem.* **275,** 17556–17560
12. Widengren, J., Mets, Ü., and Rigler, R. (1995) *J. Phys. Chem.* **99,** 13368–13379
13. Magde, D., Elson, E. L., and Webb, W. W. (1974) *Biopolymers* **13,** 29–61
14. Beechem, J. M., Gratton, E., Ameloot, M., Knutson, J. R., and Brand, L. (1991). in *Topics in Fluorescence Spectroscopy* (Lakowicz, J. R., ed) Vol. 2, p. 241, Plenum Press, New York
15. Schliebs, W., Saidowsky, J., Agianian, B., Dodt, G., Herberg, F. W., and Kunau, W. H. (1999) *J. Biol. Chem.* **274,** 5666–5673
16. Gouveia, A. M., Reguenga, C., Oliveira, M. E., Sa-Miranda, C., and Azevedo, J. E. (2000) *J. Biol. Chem.* **275,** 32444–32451
17. Otera, H., Setoguchi, K., Hamasaki, M., Kumashiro, T., Shimizu, N., and Fujiki, Y. (2002) *Mol. Cell Biol.* **22,** 1639–1655
18. Gould, S. J., and Collins, C. S. (2002) *Nat. Rev. Mol. Cell Biol.* **3,** 382–389
19. Gatto, G. J., Jr., Geisbrecht, B. V., Gould, S. J., and Berg, J. M. (2000) *Nat. Struct. Biol.* **7,** 1091–1095
20. Gatto, G. J., Jr., Maynard, E. L., Guerrerio, A. L., Geisbrecht, B. V., Gould, S. J., and Berg, J. M. (2003) *Biochemistry* **42,** 1660–1666
21. Hink, M. A., Bisseling, T., and Visser, A. J. W. G. (2002) *Plant Mol. Biol.* **50,** 871–883
22. Nicolay, K., Veenhuis, M., Douma, A. S., and Harder, W. (1987) *Arch. Microbiol.* **147,** 37–42